Encapsulation of quercetin-loaded β-lactoglobulin for drug delivery using modified anti-solvent method

Zahra Chavoshpour-Natanzi, Mehdi Sahihi

Encapsulation of quercetin-loaded β-lactoglobulin for drug delivery using modified anti-solvent method

Author links open overlay panelZahra Chavoshpour-Natanzi [a], Mehdi Sahihi [b]

[a] Department of Chemistry, University of Isfahan, Isfahan, 81746-73441, Iran

[b] Institute of Physics, Polish academy of Sciences, Aleja Lotnikow 32/46, 02-668, Warsaw, Poland

Abstract

Many scientists use proteins as attractive bio-availability enhancers for natural compounds and pharmaceuticals which have poor water solubility, due to their natural abundance, amphiphilic nature, and desirable biocompatibility. Here, we investigate the preparation, characterization, and application of β-Lactoglobulin (BLG) based nanoparticles for encapsulation of quercetin, systematically. We used anti-solvent method that is common for nano particle preparation of water-soluble proteins. The procedure involves partial unfolding of protein molecules, limited aggregation in the presence of anti-solvent, crosslinking via chemical linker, and refolding of the constituent monomers. The results showed that acetone anti-solvent has significant effect on accumulation of BLG-quercetin nanoparticles. Adjustment of acetone content to the value of 10% v/v (acetone/water) followed by mild evaporation led to a notable improvement in Encapsulation Efficiency (EE%) and Loading Efficiency (LE%), which raised LE to 13.9%. In addition, reducing glutaraldehyde amount to 50% of equivalent, led to toxicity reduction of the drug carrier system. The nanoparticles with a mean particle size of about 180–300 nm and semispherical appearance were approved using Atomic Force Microscopic (AFM) and Field Emission Scanning Electron Microscopy (FESEM) methods. Protein nanoparticles may be digested at different stages of the gastrointestinal tract, depending on acidity, ionic strength, or specificity of proteases (pepsin and trypsin). This study suggested that BLG as a resistant protein to peptic digestion forms nanoparticles that are digestible (compared to untreated BLG) by pepsin. As a result, satisfactory

controlled release was achieved under simulated fast condition, i.e., digestion in simulated gastric fluid (SGF) at pH = 2 and then in simulated intestinal fluid (SIF). Finally, the mechanism of drug release into the buffer environment was well-fitted by the Korsmeyear-Peppas kinetic model. The conclusions of this study may apply not only to quercetin-BLG system, but also to a wide variety of encapsulation systems involving water-soluble protein and hydrophobic target compound, with adequate LE and reduced toxicity.

Keywords

β-Lactoglubolin nanoparticles

Quercetin

Encapsulation and drug release

1. Introduction

Drug delivery systems (DDS) are developed to improve the therapeutic properties of pharmaceuticals. These systems release drug at a certain and definite place and affect the distribution and kinetics of drug release in the body (Benita, 2005). Nanoparticles (NPs) are widely used in drug delivery and have multiple advantages such as small size, controlled release, protection of drug molecules and ability to pass across the blood-brain barrier (Yun, Cho, & Park, 2013). These properties have made them superior in comparison to conventional DDS. Nanostructures including polymers, lipids, polysaccharides, and proteins have been explored as DDS. The selection of nanoparticle materials depends on several factors such as NPs size and intrinsic properties of the drug (Kreuter, 1994).

The most important challenges are nano-formulations, interaction of immune system proteins with NPs and the creation of a protein crown around them, which plays a key role in the ultimate performance of NPs. Protein based NPs have caught the interest of researchers in the recent years due to their desirable properties such as low toxicity, biodegradability, biocompatibility and possibility of preparing various formulations (Lohcharoenkal, Wang, Chen, & Rojanasakul, 2014). Protein defined charge and their hydrophilic and hydrophobic domains (Bengoechea, Peinado, & McClements, 2011) make them a good choice for nanoparticle formulations including gelatin

(Jahanshahi, Sanati, Hajizadeh, & Babaei, 2008), albumin (Kratz et al., 1997), gliadin (Ezpeleta et al., 1996) and milk proteins (Livney, 2010).

One of the most important whey proteins is β-Lactoglobulin (BLG) that is a member of the lipocalin superfamily (Nacka, Chobert, Burova, Léonil, & Haertlé, 1998). It has made up of 162 amino acids with a molecular weight of about 18.3 kDa (Ragona et al., 2003). Previous studies showed that BLG can bind and transport numerous amphiphilic and hydrophobic ligands (Apenten, Khokhar, & Galani, 2002; Divsalar, Saboury, Moosavi-Movahedi, & Mansoori-Torshizi, 2006; He et al., 2011; Ricchiuto et al., 2008). Interaction of BLG with polyphenols (Kanakis et al., 2011; Sahihi, Ghayeb, & Bordbar, 2012; Sahihi, Ghayeb, & Bordbar, 2013), phospholipids (Lefevre & Subirade, 2000), antioxidants (Sahihi, Ghayeb, & Bordbar, 2013), fatty acids (Mohammadi, Bordbar, Divsalar, Mohammadi, & Saboury, 2009), vitamin D and cholesterol (Wang, Allen, & Swaisgood, 1997), aromatic hydrocarbons (Invernizzi, Annoni, Natalello, Doglia, & Lotti, 2008) and so on has been investigated, previously. Besides, BLG demonstrates a significant resistance to peptic digestion due to its compact folded conformation and abundance of rigid β-sheets in its structure. The results of previous studies showed that only 9% of BLG is degraded after 4 h of incubation with pepsin (Teng, Li, Luo, Zhang, & Wang, 2013). On the other hand, it is much more readily degraded by trypsin in the small intestine (Sahu, Kasoju, Goswami, & Bora, 2011).

Flavonoids are a large group of phenolic components of plants. Quercetin, one of the most well-known flavonoids, has been included in the human diet for a long history and is present in various fruits and vegetables (Hertog, Hollman, & Katan, 1992). The use of quercetin has been widely related with various health benefits, including antioxidant, anti-inflammatory, antiviral and anticancer properties as well as its function to ease some cardiovascular diseases. Despite the great benefits of quercetin, it has some disadvantages such as poor water solubility, low bioavailability, chemical instability and short biological half-life which may reduce its efficiency when is used in the food and pharmaceuticals (Cai, Fang, Dou, Yu, & Zhai, 2013).

In the past decade, many studies have been done on protein NPs. Antçnio et al., prepared soy protein NPs using anti-solvent method (Antçnio, Khalil, & Mainardes, 2016). The soy protein NPs were also used to load folic acid (Teng, Luo, & Wang, 2012). The results showed better stability of folic acid compared to its free state and confirmed that 57% of the drug was encapsulated in nanoparticles. Reduction of particles size and increasing the amount of drug loading are important

in NPs preparation. Therefore, they synthesized soy protein-polysaccharide complexes that could improve the properties of soy protein NPs. The results showed that vitamin D loading capacity was about 80.5%–90.5% and the size of particles was around 162–243 nm. Also, the formed complex showed good stability in the various ranges of pH (Teng, Luo, Wang, Zhang, & Wang, 2013). Rahiminejad et al., developed the bovine serum albumin (BSA) protein nanoparticles and evaluated different conditions such as pH, temperature, and initial protein concentration to achieve suitable particle size (Rahimnejad, Jahanshahi, & Najafpour, 2006). Recent studies led to the preparation of BLG NPs and loading of various drugs into it due to its unique structure and function as an ideal carrier to transport of bioactive molecules. Recently, curcumin was encapsulated into the BLG NPs and was examined in different conditions of anti-solvent content, the amount of crosslink agent and various ratios of curcumin/BLG NPs. Also, the release of the drug in simulated gastric fluids (SGF) and simulated intestinal fluids (SIF) was investigated. The results showed that encapsulated curcumin has better resistance to digestion than free curcumin (Teng, Li, & Wang, 2014).

The anti-solvent method is one of the most common methods to prepare the Nps of proteins that are soluble in water and unstable in some organic solvents (a wide range of albumins and globulins). However, this method has drawbacks that limit its using. For example, the loading efficiency of the prepared protein NPs is mostly lower than the other methods. The second weakness lies in toxicity of chemical materials that are necessary for NPs preparation. The presence of glutaraldehyde and acetone as a cross-linker and anti-solvent, respectively, are concerns for the safety of this method (Ezpeleta et al., 1996). The anti-solvent method contains four steps, i.e., preparation of protein solution; acetone addition; glutaraldehyde addition and evaporation. In the recent studies, the typical protocol for preparation of protein NPs was modified due to increase the amount of curcumin loaded into protein NPs and reduce the toxicity of DDS (Teng, Li, & Wang, 2014).

The physical and chemical properties of the used protein and drug have various effects on the preparation and characteristics of NPs. In fact, the formation of nanoparticles depends on increasing of protein unfolding and decreasing its hydrophobic intramolecular interactions. During the formation of the nanoparticles, the protein undergoes conformational changes depending on its composition, concentration, crosslinking agent and preparation conditions such as pH, ionic strength and type of the solvent (D'Mello, Das, Das, Pathak, & Thassu, 2009). Also, a drug can be

loaded either by encapsulation inside the nanoparticle or by interaction with the protein through covalent or noncovalent interactions. It is well known that the loading rate of the drug in nanoparticles, will affect on the physical and chemical properties of the drug (Vandervoort & Ludwig, 2004). Therefore, our purpose is fabrication of small nanoparticles with narrow size distribution as a carrier for DDS. BLG can be used for the development of protein NPs due to its importance as a suitable drug carrier. In the present paper, we used the modified anti-solvent method for preparation of BLG NPs in different conditions such as pH, acetone content, initial protein concentration and quercetin/BLG ratios. Then, it was introduced as a DDS to transfer of quercetin; and the release of quercetin in SGF and SIF was also investigated.

2. Materials and methods

Materials. Bovine BLG (90% purity), pepsin (3200–4500 units/mg protein), trypsin (10000 units/mg protein), and quercetin (98% purity) were purchased from Sigma-Aldrich (St. Louis, MO, USA). Potassium hydrogen phosphate, potassium dihydrogen phosphate, hydrochloric acid, sodium acetate, acetic acid, sodium hydroxide, acetone, ethanol, tween 80 and glutaraldehyde were purchased from Merck chemical Co. All of the chemicals were analytical grade and were used without further purification.

2.1. Preparation of quercetin-loaded BLG NPs

BLG NPs were prepared by modified desolvation method (Teng, Luo, & Wang, 2012). The whole process was done in 800 rpm constant stirring. BLG was dissolved in deionized water at 5, 10 and 15 mg/ml and quercetin was dispersed in acetone at 2 mg/ml, and were equilibrated for 1 h. Pure acetone was added dropwise to BLG dispersion (Up to 1.5-fold of the initial volume of BLG solution) and an appropriate amount of quercetin solution was added to achieve 5, 10, and 15%, w/w quercetin/protein ratios. Additional pure acetone was then added to total volume of 10 mL to decrease the particle concentration (Weber, Coester, Kreuter, & Langer, 2000) and the solutions were equilibrated for 30 min. The final content of acetone before crosslinking was about 95% v/v. Two levels (50, and 100% equivalent) of glutaraldehyde as a chemical cross-linker were applied. Theoretically, each milligram of BLG needs 40 µg glutaraldehyde for stoichiometric crosslinking (Teng, Li, Luo, Zhang, & Wang, 2013). After 16 h of crosslinking, various solutions with final acetone content ranged from 10 to 90% v/v were prepared. It can be inferred that the evaporation

process with continuous decreasing in acetone content, may be critical for encapsulation of quercetin. Hence, after 1 h of equilibration, the acetone was evaporated slightly at room temperature under reduced pressure using a vacuum oven (Frapajoohesh, IRAN) to remove acetone. Evaporation step lasted about 3 h and additional water was then added to achieve a final volume of 5 mL. The final dispersion was stored at 4 °C for further analyzes. The initial and final pH values of the dispersions were about 7.

2.2. Quantitative analysis

For quantitative analysis; the BLG-quercetin NPs were prepared based on the above procedure. Also, 100% equivalent of glutaraldehyde was used and mixed with aqueous acetone to achieve various acetone contents. After equilibration for 1 h, the dispersion was centrifuged (9000 g, 30 min, room temperature). The insoluble quercetin was recovered in the precipitate and dissolved in pure acetone, whereas the supernatant was subjected to ultrafiltration by centrifugation (5000 g, 15 min, room temperature) using a Macrosep centrifuge tube (MW cutoff 10 kDa; Pall Corp., Ann Arbor, MI, USA). The filtrate containing non-bound quercetin was recovered and diluted with pure acetone. The concentrations of the subsequent mixtures were measured using UV–Vis spectroscopy (Lambda 265, PerkinElmer) at $\lambda = 375$ nm.

2.3. Characterization of quercetin-loaded BLG NPs

Surface charge, size and morphology of BLG NPs were measured using Zeta potential (ZP) and DLS (dynamic light scattering) (HORIBA SZ-100) or AFM (Dualscop C-26, DME Germany) methods, respectively. Particle size and surface charge determination are essential for appropriate characterization of NPs. DLS and ZP measurements have gained popularity as simple, easy and reproducible methods to determine particle size and surface charge, respectively. AFM method was used under tapping mode to measure the topological shape of BLG NPs. The prepared BLG NPs were spread and dried onto Lamel surface. Sample topologies were generated by recording the vertical movements during scanning and the particle images were analyzed with the DME-SPM software.

The quercetin-loaded BLG NPs were characterized by Fourier-transform infrared (FT-IR) and X-ray diffraction (XRD) analyses. Samples were freeze-dried and mounted onto a Jasco FT/IR 6300 spectrometer (Jasco Inc., Easton, MD, USA). The infrared transmittance was recorded at

wavenumbers between 1000 and 4000 cm^{-1}. At least 100 scans were undertaken for each sample. The spectra were averaged, smoothed, and corrected for their baselines using Spectra Manager software. Also, XRD patterns of pure quercetin, quercetin-loaded BLG NPs and blank BLG NPs were obtained using the X-ray diffract meter (D8 ADVANCE, Germany) with Ni-filtered Cu K_α radiation. The measurements were performed at a voltage of 40 kV and 25 mA. Scanning electron microscopy (SEM) was used to observe the morphology of the nanoparticles. Approximately 40 μL of the dispersion (after evaporation and water supplementation) was cast dried on an aluminum pan, mounted on a conductive carbon tape, coated with gold/platinum using a sputter coater, and observed under SEM (MIRA3TESCAN-XMU).

2.4. Encapsulation Efficiency (EE%) and loading efficiency (LE%)

The EE for each sample was calculated after concentration determination of insoluble and free unbounded quercetin (please see section 2.2) as follows (Teng, Luo, & Wang, 2012):

$$EE\% = 100 - \frac{amount\ of\ precipated\ quercetin}{\text{total amount of quercetin}} \times 100 \quad (1)$$

In addition, after the ultrafiltration by centrifugation mentioned above, the retentate containing the quercetin-encapsulated nanoparticles was collected and lyophilized. The LE was calculated as follows:(2)Weight of encapsulated quercetin = total amount of quercetin - (non-bound and precipitated quercetin)

$$LE\% = \frac{\text{weight of encapsulated quercetin}}{\text{total weight of NPs}} \times 100 \quad (3)$$

2.5. In vitro release of quercetin

Release in PBS. Prepared samples with the following parameters were chosen for in vitro release study: quercetin loading of 10, and 15% (w/w), initial acetone content of 10% (v/v) and glutaraldehyde levels that showed the optimal EE for each quercetin loading ratio. Samples were taken after evaporation but prior to supplementation of water. All of the used buffers (PBS, SGF and SIF) contained 5 mg/mL Tween 80. Also, the PBS was prepared at pH = 7.2 and 0.1 mol/L of phosphate salts. Two milliliters of the above mentioned samples was mixed with 2 mL of PBS and incubated at 37 °C for 30 min. The mixture was injected into a sealed dialysis tube (MW

cutoff = 10 kDa), which was then placed in a flask containing 60 mL of PBS (preheated at 37 °C). The flask was then incubated in a reciprocal shaking bath at 37 °C under constant shaking at 120 rpm. At predetermined time intervals, aliquots of 2 mL were withdrawn from the flask and measured for absorbance at 375 nm, which was converted to the mass of released quercetin.

Release in SGF and SIF. The nanoparticle dispersion with quercetin loading of 10% was chosen for this study. Two milliliters of the sample were incubated at 37 °C and then were diluted with 4 mL of two preheated buffers, i.e., SGF-2 or SGF-5 (same as SGF-2 but its pH was adjusted to 5.0). These buffers mimicked the gastric environment at fasting and fed states, respectively (Fotaki & Vertzoni, 2010). SGF and SIF were prepared based on previously published methods (Marques, Loebenberg, & Almukainzi, 2011; Remondetto, Beyssac, & Subirade, 2004; Teng, Li, & Wang, 2014) and BLG/protease ratio was about 100:1. After 15 min of mixing, the dispersion was subjected into a dialysis bag and was placed in a flask containing 20 mL of SGF without pepsin enzyme. At predetermined time intervals, aliquots of 2 mL were withdrawn from the flask and measured for absorbance at $\lambda = 375$ nm, which was converted to the mass of released quercetin. On the other hand, another batch of the nanoparticle dispersions were mixed with SGF-2 and digested for 60 min at 37 °C in the reciprocal shaking bath. It was then mixed with SIF buffer and eventually injected into the dialysis bag. Afterwards, the dialysis bag was placed in 20 mL SIF flask without trypsin enzyme and the absorption of released quercetin was measured using UV–Vis spectroscopy method.

3. Results and discussion

3.1. Concentration effect on the size, shape and stability of BLG NPs

In this study, BLG solutions with initial concentrations of 5, 10 and 15 mg/mL were used to prepare the NPs with size of 180–298 nm. The results of DLS method are presented in Table 1. The results show that, smaller BLG NPs can be obtained in 10 mg/mL initial protein concentration. Zeta potential allows us to study the stabilization of colloidal systems. The stability of the colloidal suspensions of nanoparticles depends on the charged species present at the particle surface that impair the aggregation and the consequent collapse. Since the stability of the colloidal system is due to the balance between the attractive and repulsive forces; the system will be stable when the repulsive forces are stronger. This stability may be achieved through steric repulsions or

electrostatic interactions. Usually, it is accepted that the zeta potential between −30mV and +30 mV indicates an unstable suspension, while for values higher than +30 mV or lower than −30mV it is assumed that you have a stable system (Bhattacharjee, 2016). Zeta potentials of BLG NPs at different initial protein concentrations were evaluated and the results showed that the initial protein concentration of 10 mg/mL makes the most stable NPs with ZP of about −85.8 mV (Table 1).

Table 1. DLS and Zeta potential Data for BLG NPs at 100% glutaraldehyde.

Initial protein concentration (mg/mL)	[Quer]/[BLG] (w/w)	Particle size	Zeta potential (mV)
5	–	298.9 ± 41.5	−32.3
10	–	152.3 ± 26.4	−85.8
15	–	180.6 ± 7.1	−71.7
10	5%	250.9 ± 21.5	−64.7
10	15%	268.8 ± 34.4	−63.5

The effect of drug concentration on the size of DDS was also evaluated. In the presence of 5% and 15% (w/w) of quercetin/BLG, the particle size was increased, which was reasonable. According to the ZP data, stability of the system is reduced after loading of the drug, which can be due to the presence of quercetin on the surface of the NPs and reducing the surface charge. AFM images also showed that the nanoparticles were formed by smooth surface and semispherical shape (Fig. 1, Fig. 2). Previous studies revealed that the smaller nanoparticles have higher stability than the larger ones and can escape from the vascular system via cavities in the lining of blood vessel (Müller, Leuenberger, & Kissel, 1996).

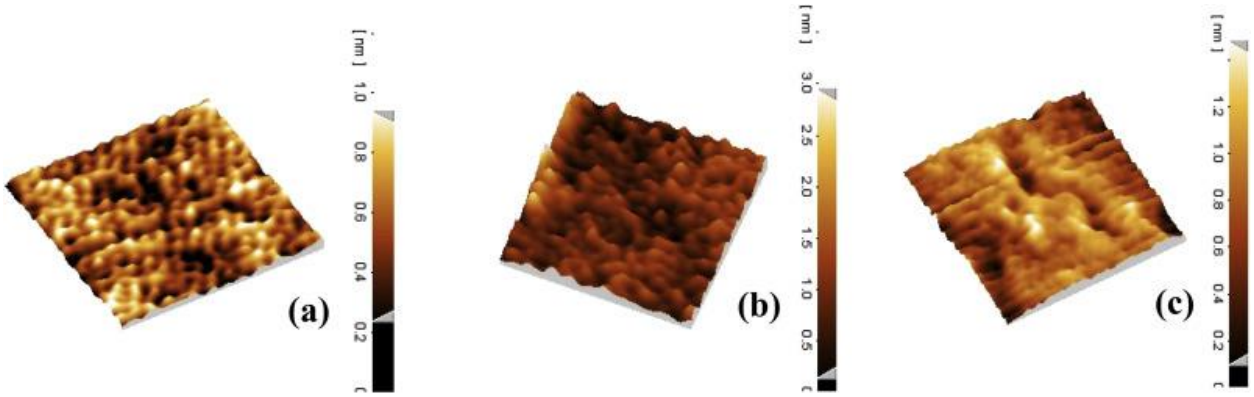

Fig. 1. AFM images of BLG NPs with initial protein concentration of: a) 5 mg/mL b) 10 mg/mL c) 15 mg/mL.

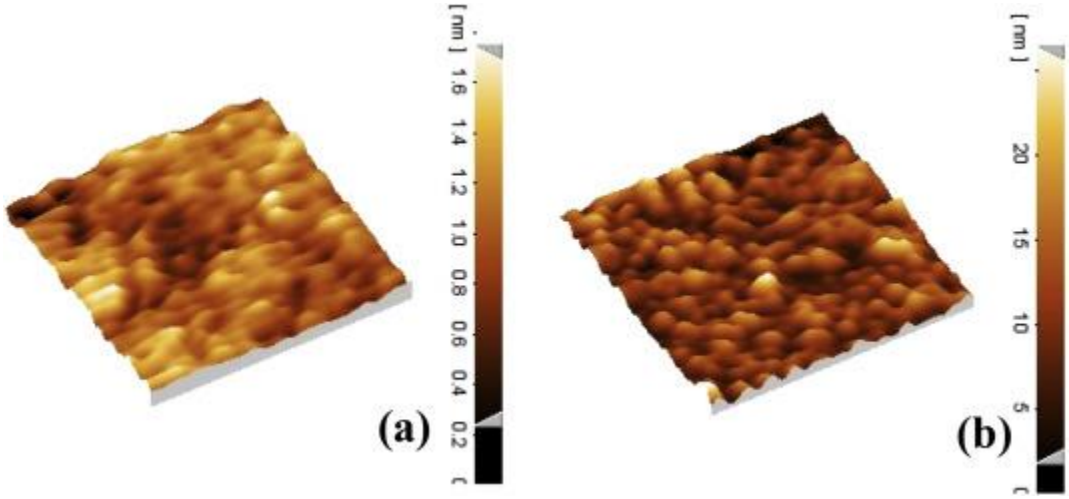

Fig. 2. AFM images of BLG NPs with 10 mg/mL initial protein concentrations for: a) 5%w/w quercetin/BLG NPs b) 15%w/w quercetin/BLG NPs.

3.2. pH effect

After particle size optimization in 10 mg/mL of initial protein concentration; the pH effect on morphology of BLG NPs was evaluated. In fabrication of protein NPs, both gravity and repulsive forces exist between particles, and balance between these forces produces nanoparticles of a certain shape. Due to dependence of both gravity and repulsive forces on pH (Sahihi, Bordbar, Ghayeb, & Fani, 2012), the shape of BLG NPs is significantly affected by pH value of the aqueous solution. AFM imaging results indicated that protein nanoparticles at pH = 4 and 9 do not have the semispherical appearance. Hence, the pH = 7 was selected as optimized pH due to importance of NPs morphology (Fig. 3).

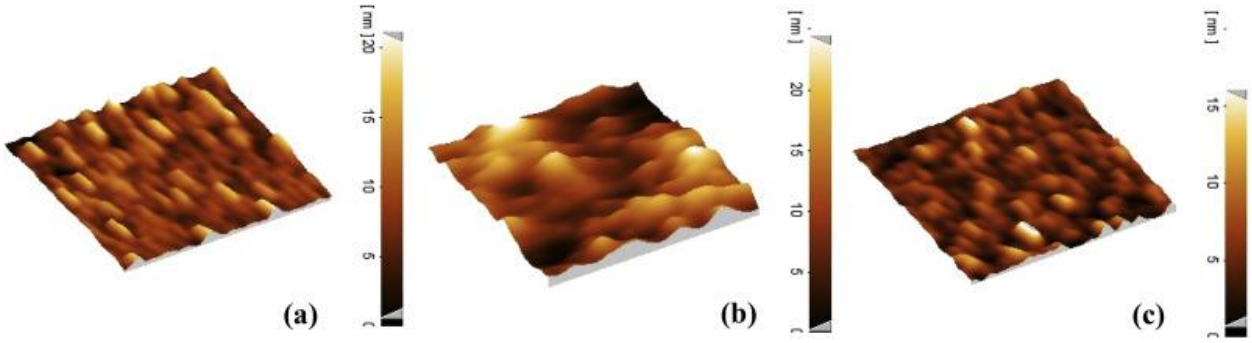

Fig. 3. AFM images of BLG NPs at different pHs: a) pH = 4 b) pH = 7 c) pH = 9.

3.3. Characterization of quercetin-loaded NPs

The SEM images of BLG NPs are shown in Fig. 4. FESEM images exhibit particles with smooth surface and semispherical shape. Two main groups of particles were identified in the images, i.e., larger particles with an average particle size of about 200 nm and smaller particles with size of about 40–50 nm (Fig. 4). Fig. 4 demonstrates that the former type of particles was possibly assembled from the latter one. Such aggregates might have existed in the nanoparticle dispersion before drying process.

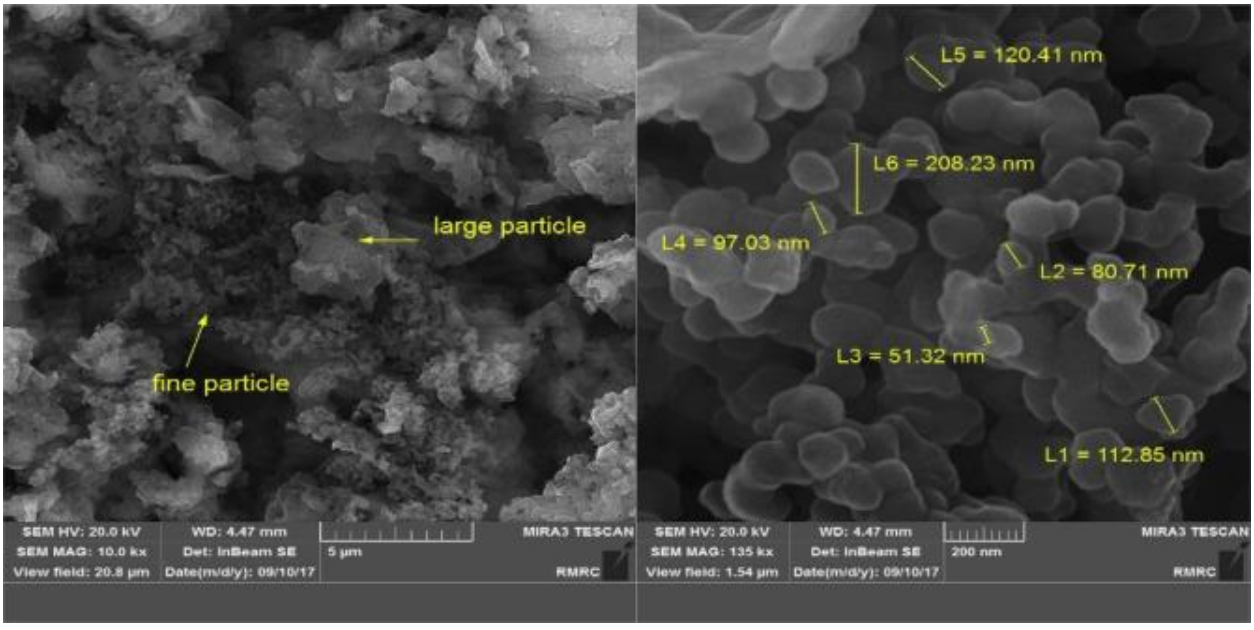

Fig. 4. FESEM images of quercetin-loaded BLG nanoparticles (coexistence of larger and smaller particles).

The structural characteristics of food proteins are often studied by Fourier transform infrared (FT–IR) spectroscopy in order to determine their structure–function relationship. Each compound has a characteristic set of absorption bands in its infrared spectrum. Characteristic bands found in the infrared spectra of proteins and polypeptides include the Amide I and Amide II which arise from amide bonds. The absorptions related to Amide I and Amide II bands lead to stretching vibrations of C=O and bending vibrations of the N–H bonds, respectively. Locations of the both bands are sensitive to the secondary structure contents of a protein due to their role in hydrogen bonds that are formed between different elements of protein secondary structure (Byler & Susi, 1986; Surewicz & Mantsch, 1988).

In the present work, quercetin loading into BLG NPs in 15% (w/w) quercetin/BLG was investigated using FT-IR method. Fig. 5 shows 4.4 nm and 12 nm shift of Amide I (1654.2 cm^{-1}, C = O stretching) and amide II (1522.52 cm^{-1}, NH bending and CN stretching) bands of BLG NPs in the presence of quercetin, respectively. These changes suggest that carbonyl or amine groups of protein chains play key role in protein-quercetin interaction. In addition, the broad region in about 3300 cm^{-1} (OH-group) and its changed intensity in the presence of quercetin, suggests formation of hydrogen bonds between the protein and quercetin (loading quercetin into BLG NPs) (Teng, Luo, & Wang, 2012). On the other hand, encapsulation of quercetin with high ratio of quercetin to BLG (100:1) removes the quercetin peaks in FT-IR spectrum of the quercetin-NPs complex.

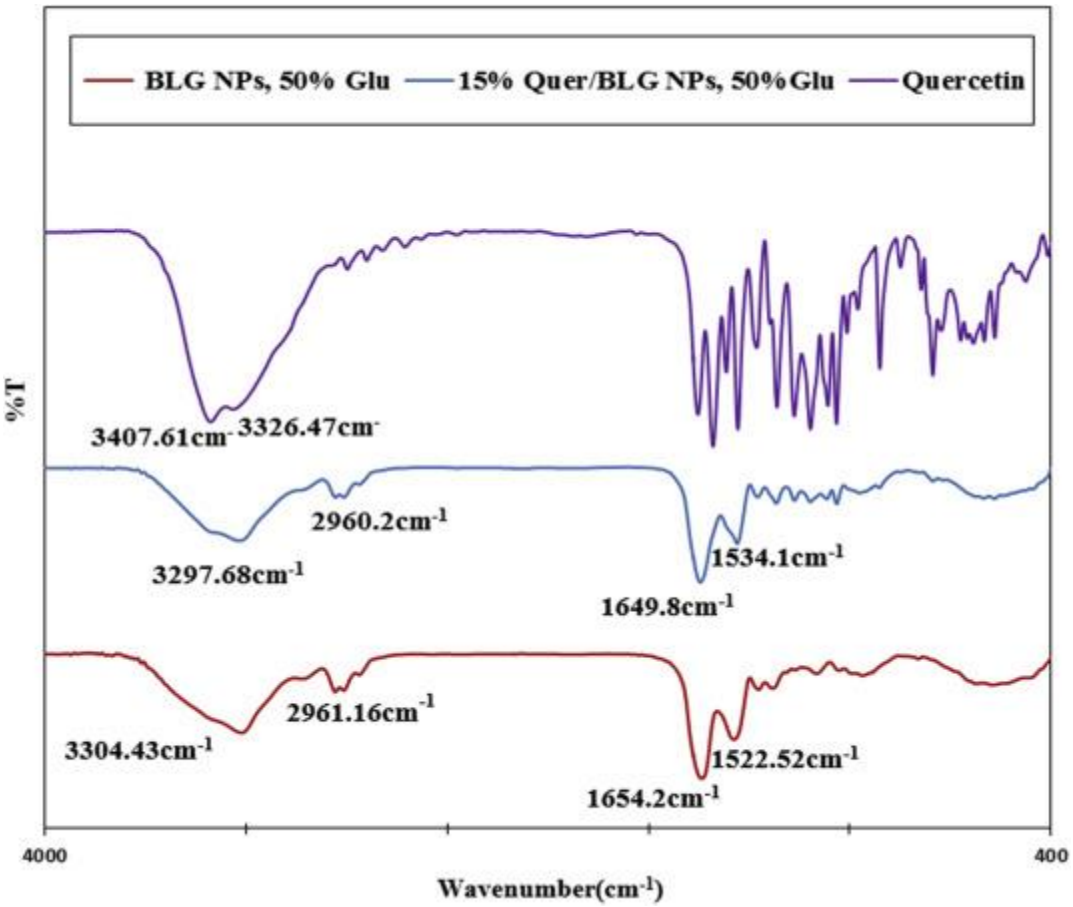

Fig. 5. FT-IR spectra of empty BLG NPs, quercetin/BLG NPs and quercetin. The amide I band (between 1600 and 1700 cm^{-1}) is mainly due to C=O stretching vibration and is directly related to the backbone conformation. Amide II (between 1500 and 1600 cm^{-1}) comes from the N–H bending vibration.

Solid substances may reveal crystalline and/or amorphous characteristics. XRD method can distinguish systems/materials between crystalline and amorphous, effectively. The crystalline substances present with defined peaks despite of the amorphous compounds (Patel, Patel, Chakraborty, & Shukla, 2015). In general, amorphous solids are more soluble than crystalline forms due to free energy of dissolution process. Amorphous solids have randomy arranged molecules, so low power consumption is required to separate them. Accordingly, their rate of dissolution is faster than crystal form (Riekes et al., 2011). The XRD patterns of quercetin, blank BLG NPs and quercetin-loaded BLG NPs are given in Figs. 6 and S1. Quercetin shows defined peaks at angles 7°, 8°, 12.5°, 14°, 18°, 29° and 32° which are characteristics of crystalline structure

(Fig. 1(a)), while, BLG bands do not show any peaks due to its amorphous nature (Fig. S1 (b)). Fig. 6 reveals that the intensity of quercetin peaks is decreased in quercetin-BLG NPs complex. One explanation is that quercetin molecules were encapsulated or dispersed in the polymer matrix during the desolvation process (Wu et al., 2008).

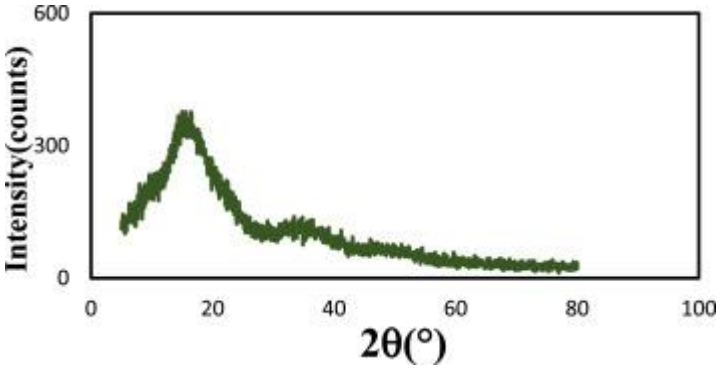

Fig. 6. X-ray powder diffraction of quercetin-loaded BLG NPs.

3.4. Binding of quercetin to BLG NPs as a function of acetone content

In water/acetone binary system containing BLG NPs, quercetin molecules could be find in three forms, i.e., insoluble quercetin, dissolved quercetin and BLG-bound quercetin molecules that were measured in the precipitate, filtrate and retentate, respectively. Fig. 7 shows the distribution of quercetin in BLG NPs as a function of acetone content. The data were obtained after rapidly diluting the cross-linked dispersion with appropriate water/acetone mixtures. As can be seen from this figure, the percentage of free quercetin was increased significantly at acetone content >40% v/v. The results were similar to a relevant study on BLG monomers, which reported that the refined binding capability were decreased by 30% or higher concentration of ethanol (Duclairoir, Nakache, Marchais, & Orecchioni, 1998; Dufour & Haertl', 1990). The results suggest a weak interaction between the ligand and BLG NPs. On the other hand, 30–40% of quercetin molecules were detected in the precipitate in the presence of 10–25% acetone. This observation was probably due to: (i) quercetin as a hydrophobic compound exhibits low solubility in 10–25% acetone and (ii) most of the protein molecules were partly or fully folded, so there were insufficient hydrophobic sites to associate with quercetin. (Teng, Luo, & Wang, 2012). In addition, most of the ligand binding sites lose their activity at high level of acetone during preparation of the NPs

(Zhang et al., 2013). Therefore, the quercetin-BLG association might have taken place mostly on the hydrophobic sites exposed by desolvation, rather than the native binding sites of BLG.

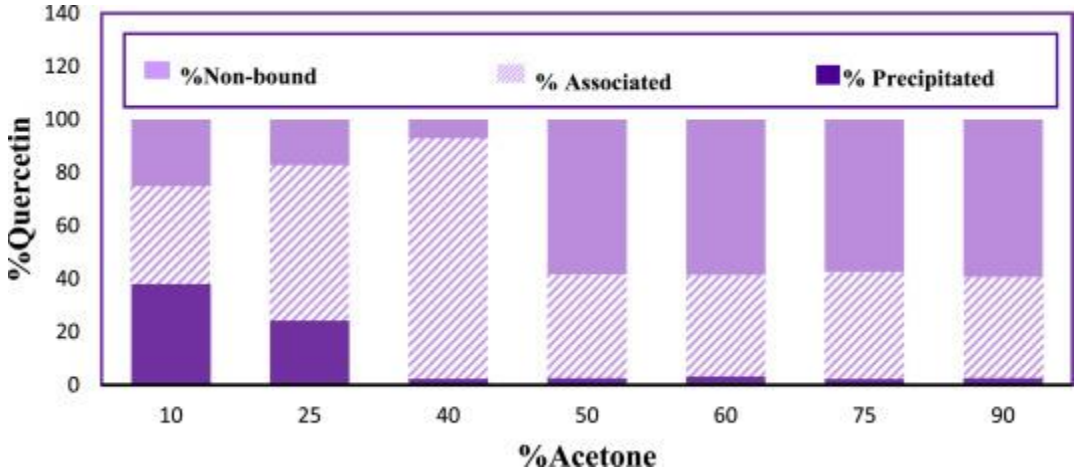

Fig. 7. Effect of acetone content on the distribution of quercetin in BLG NPs dispersion. BLG concentration was 10 mg/mL, quercetin concentration was 1 mg/mL and the nanoparticles were cross-linked with 100% equivalent of glutaraldehyde.

In 40% of acetone, a considerable percentage of quercetin molecules (90%) are in protein associated form. This phenomenon is possibly due to two factors: (i) the high polarity of 40% acetone compared to higher concentrations, force quercetin molecules to associate with other hydrophobic molecules (BLG) and minimize their contact with water, (ii) a great number of hydrophobic sites on BLG molecules are exposed in 40% acetone in comparison with 25% acetone (Teng, Luo, & Wang, 2012), which cause the association and stabilization of more quercetin molecules.

Due to the acetone content dependence of quercetin distribution, it can be judged that the evaporation process is critical for encapsulation of quercetin. We hypothesized that the LE of BLG NPs might be improved by lowering the acetone content after crosslinking and equilibrating the dispersion for a period of time to allow sufficient quercetin-BLG binding. Hence, the dispersion should be evaporated mildly.

3.5. Effect of acetone content and glutaraldehyde level on EE% and LE%

The EE of quercetin-loaded BLG NPs as a function of acetone content and glutaraldehyde levels was investigated. Fig. 8 reveals that the change in EE does not show a direct and regular relationship with acetone content. However, it can be realized that in all cases, the highest amount of EE is observed in 90% and/or 10% of acetone. These irregular changes are observed in both values of 50% and 100% equivalents of glutaraldehyde. All of the EE values refer to initial concentrations of the drug in various acetone contents and different levels of glutaraldehyde have been presented in Table 2. The results show the similar changes for the values of LE, too.

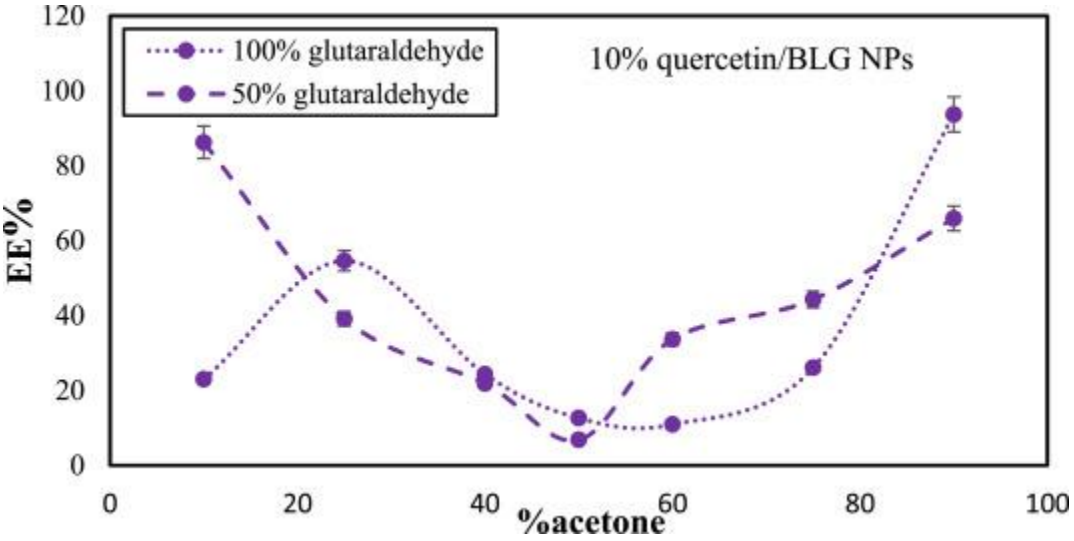

Fig. 8. Effect of acetone and glutaraldehyde contents on the EE% of quercetin/BLG NPs at 10% of quercetin/BLG mixing ratio.

Table 2. Characteristics of quercetin-loaded BLG nanoparticles at 10% quercetin/BLG mixing ratio.

acetone%	100%glu EE%	LE%	50%glu EE%	LE%
10	78.8 ± 1.102	8.7 ± 0.123	86.1 ± 1.54	9.5 ± 0.171

acetone%	100%glu EE%	LE%	50%glu EE%	LE%
25	54.6 ± 0.307	6.1 ± 0.034	39.1 ± 0.302	4.3 ± 0.033
40	24.3 ± 0.598	2.7 ± 0.067	21.7 ± 0.548	2.4 ± 0.061
50	12.6 ± 0.392	1.4 ± 0.044	6.8 ± 0.193	0.7 ± 0.022
60	10.9 ± 0.127	1.2 ± 0.014	33.7 ± 0.121	3.7 ± 0.013
75	26.1 ± 0.202	2.9 ± 0.022	44.3 ± 0.107	4.9 ± 0.012
90	93.6 ± 0.520	10.4 ± 0.006	65.9 ± 0.054	7.3 ± 0.006

At 90% of acetone and 100% of glutaraldehyde, the LE values were about 13.9%, 10.4% and 4.9% for the nanoparticles mixed with 15%, 10% and 5% (w/w) quercetin/BLG NPs, respectively. Regarding to the maximum amount of EE in 90% of acetone, it can be suggested that this loading capacity is due to high solubility of quercetin in acetone as well as trapping large number of quercetin molecules during the evaporation process at hydrophilic sites and their encapsulation. The samples containing 10% of acetone showed the LE values about 11.9%, 8.7% and 3.7%, for 15%, 10% and 5% w/w quercetin/NPs, respectively. As a result, all soluble quercetin (free and encapsulated) have been inserted into the capsules due to the high solvent polarity and leads their strong interactions with BLG NPs.

On the basis of these results, adjustment of the lowest acetone content is critical for achieving the optimal values for LE and EE. Moreover, a lower glutaraldehyde levels could be applied for preparation of BLG NPs. As it is shown in Figs. 8 and 50% and 100% of glutaraldehyde levels were investigated for all of the quercetin/BLG NPs ratios and acetone contents (the results related to 5% and 15% (w/w) of acetone are shown in Table S1 and Fig. S2). Table 2 shows that at 50% of glutaraldehyde, EE% for samples with 10% and 90% of acetone were higher than 100% of glutaraldehyde, or had a few difference. In fact, by decreasing the glutaraldehyde level, with the highest EE values, the toxicity of drug delivery system can be reduced, effectively.

3.6. In vitro release of quercetin from BLG NPs

In PBS: Fig. 9(a) shows release of quercetin from BLG NPs in a PBS/Tween 80 system. It is remarkable that quercetin degrades rapidly in PBS, but its stability could be greatly improved in the presence of nonionic surfactants such as Tween 80 (Tønnesen & Karlsen, 1985). Two systems were chosen to investigate quercetin release in PBS buffer system based on the EE and LE values in previous section. These conditions consist of 50% of glutaraldehyde, 10% of acetone content, and 10% and 15% w/w of quercetin/BLG NPs. The results indicate that release rate for nanoparticles with low quercetin loading is higher than the other case with high quercetin loading due to the following reasons: (i) the particles with higher quercetin loading exhibit greater sizes, and have lower quercetin specific surface area (ii) solubility of quercetin in the PBS/Tween 80 system is constant in a given environment and desolvation of quercetin is slowed as its concentration reaches to the equilibrium value; and (iii) higher loading indicates higher concentration of quercetin accumulated in the outer buffer, which slows the diffusion of quercetin through the dialysis membrane.

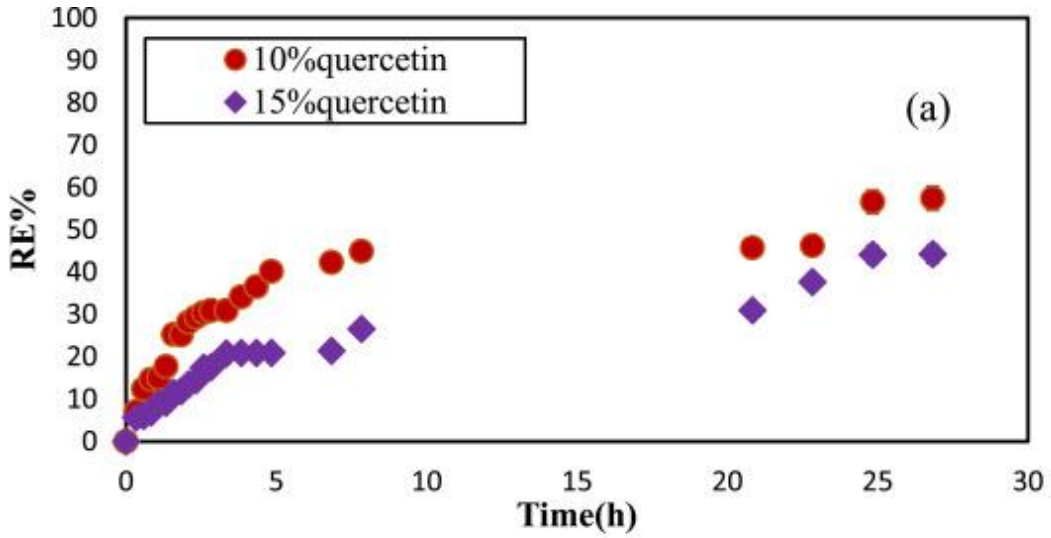
10%quercetin
15%quercetin
(a)
RE%
Time(h)

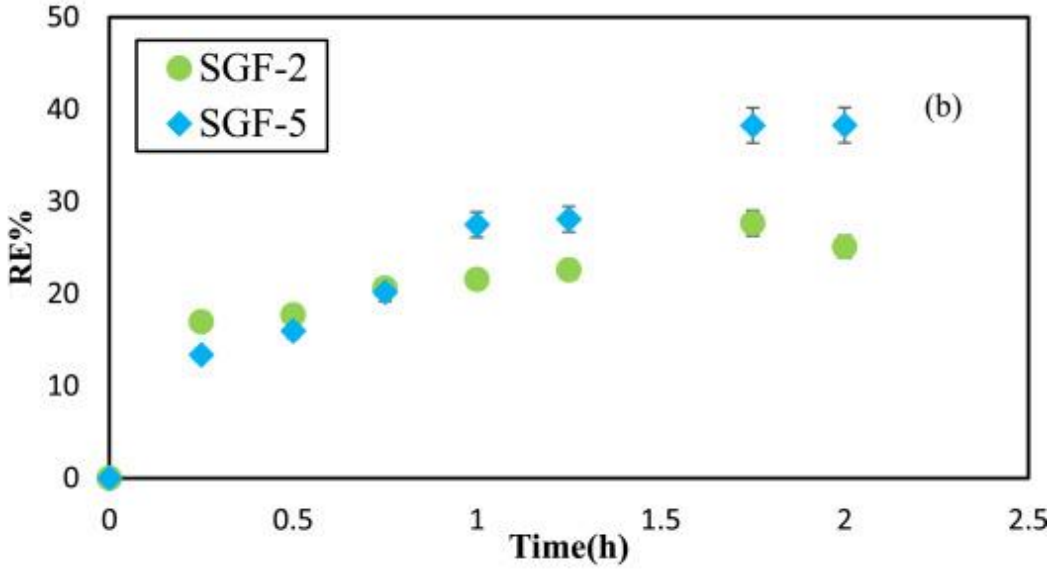
SGF-2
SGF-5
(b)
RE%
Time(h)

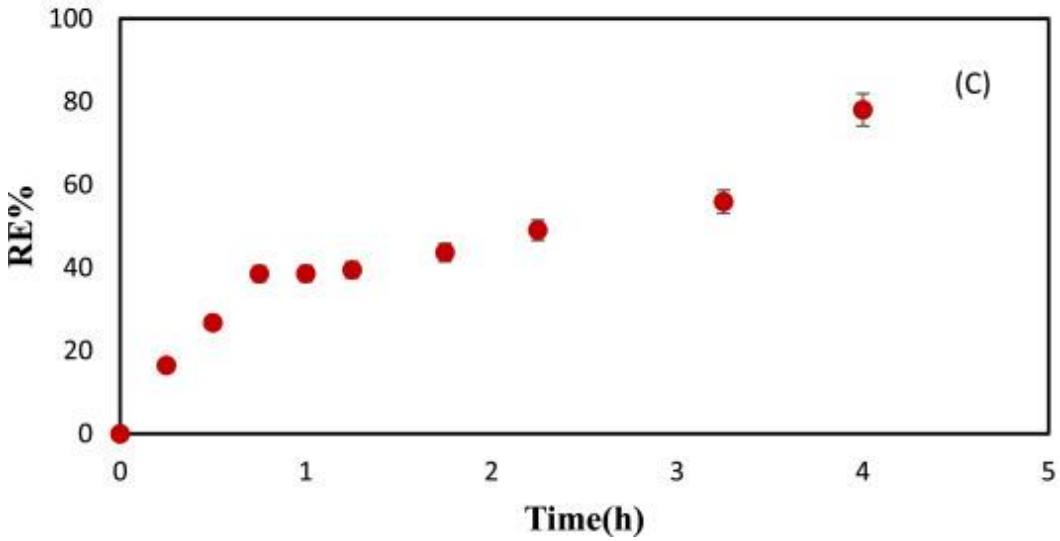
(C)
RE%
Time(h)

Fig. 9. Time-dependent release of quercetin from BLG nanoparticles in a) PBS/Tween 80 buffer, DDS consists of 50% glutaraldehyde, 10% acetone content, and 10% and 15% w/w, quercetin/BLG NPs in, b) SGF-2 and SGF-5, DDS consists of 50% glutaraldehyde, 10% acetone content, and 10% quercetin/BLG NPs and c) SIF, DDS consists of 50% glutaraldehyde, 10% acetone content, and 10% quercetin/BLG NPs.

3.7. In vitro drug release kinetics

In this study, five kinetic models have been used to investigate the mechanism of quercetin release from BLG NPs, which are briefly described as below:

- i)

  Zero order kinetics model follows the equation as $(Q_t/Q_0) = k_0t$, where k_0 is the zeroth order rate constant; Q_t denotes the amount of released quercetin and Q_0 denotes the initial amount of quercetin. In this model the drug release is independent of its concentration (Najib & Suleiman, 1985).
- ii)

  First order kinetics model follows the equation as $\text{Ln}\ (Q_t/Q_0) = -k_1t$, where k_1 is the first order rate constant. The release rate is concentration dependent (Desai, Singh, Simonelli, & Higuchi, 1966).
- iii)

  Korsmeyer-Peppas model follows the equation as $Q_t/Q_\infty = kt^n$ where Q_t/Q_∞ is fraction of released drug at time t, k is the release rate constant and n is the release exponent. The n value is used to characterize different release for cylindrical shaped matrices (Korsmeyer, Gurny, Doelker, Buri, & Peppas, 1983).
- iv)

  Hxson-Crowell model follows the equation as $Q^{1.3} = -k_st$ where k_s is constant incorporating the surface volume relation (Hixson & Crowell, 1931).
- v)

  Higuchi model follows the equation as $Q/Q_0 = k_H.t^{1.2}$ where k_H is Higuchi matrix release kinetics constant. The drug release from matrix is directly proportional to square root of time and is based on the Fickian diffusion (Higuchi, 1963).

The quercetin release in PBS for 5%, 10% and 15% (w/w) quercetin/BLG NPs were investigated by all five kinetic models, and the related results are shown in Fig. S3 and Table 3. The R^2 values for Korsmeyer-Peppas model (Fig. 3(c)) are slightly higher than the other models and show its better performance to predict the quercetin release from the NPs. In this model, if the n value is 0.45, the release follows the Fickian diffusion mechanism. If n is between 0.45 and 0.89, polymer matrix loss is effective in drug release and finally, if the value of n is 0.89; releasing is time independent. Hence, the polymer matrix loss is effective in the present case according to the amount of n = 0.57, 0.57 and 0.49, for 5%, 10% and 15% (w/w) samples, respectively (Higuchi, 1963).

Table 3. Curve fitting of quercetin release profile from BLG NPs.

[Quer]/[BLG]	**5%**		**10%**		**15%**	
Kinetic Model	**k**	**R^2**	**k**	**R^2**	**k**	**R^2**
Zero order	0.0002 (mg/h)	0.7145	0.0003 (mg/h)	0.6064	0.0005 (mg/h)	0.8214
First order	0.0264 (mg/h)	0.6189	0.0217 (mg/h)	0.6786	0.0160 (mg/h)	0.8552
Korsmeyer-peppas	1.3674 (h)	0.9659	1.5240 (h)	0.9517	1.2153 (h)	0.9543
Hixson-Crowell	0.0001 ($mg^{1/3}$/h)	0.7084	0.0001 ($mg^{1/3}$/h)	0.6064	0.0002 ($mg^{1/3}$/h)	0.8214
Higuchi	0.0027 ($mg/h^{1/2}$)	0.8373	0.0023 ($mg/h^{1/2}$)	0.7914	0.0029 ($mg/h^{1/2}$)	0.9347

In SGF and SIF: The release profiles of quercetin in simulated gastric fluids (SGF) and simulated intestinal fluids (SIF) are shown in Fig. 9. The releasing profile for nanoparticles with 10% of quercetin loading was chosen for SGF and SIF experiments, due to its higher releasing rate than 15% (w/w) in PBS.

Releasing in SGF was investigated at two different pHs: pH = 2 that represents the gastric condition in the fasting state and pH = 5 that corresponds to the fed state (Fotaki & Vertzoni, 2010). After 1 h of digestion, the mixture was transferred to SIF to determine the release profile under the simulated intestinal condition. It was noteworthy that after 2 h, about 40% of encapsulated quercetin was released in SGF at pH = 5 (Fig. 9(b)). BLG is known for its resistance to peptic digestion that is its major advantage over other proteins with respect to the transportation and delivery of nutraceuticals and drugs (Reddy, Kella, & Kinsella, 1988). This characteristic was confirmed by Teng and et al., in which only 9% of BLG was degraded after 4 h of incubation with pepsin (Teng, Li, Luo, Zhang, & Wang, 2013; Otte, Zakora, Qvist, Olsen, & Barkholt, 1997). We hypothesized from this result that the BLG NPs were actually decomposed in SGF at pH = 5, although the individual BLG molecules remained intact. When NPs were dispersed in SGF at pH = 2 (Fig. 9(b)), the BLG NPs exhibited significantly lower rate of release than at pH = 5, and 25% of encapsulated quercetin being released in 2 h. After being transferred to SIF (Fig. 9(c)), the remaining quercetin molecules continued to release from the nanoparticles. This was probably due to degradation of residual BLG NPs as well as the molecules, because of the known capability of trypsin to digest BLG (Otte, Zakora, Qvist, Olsen, & Barkholt, 1997). The significant difference in the releasing pattern of dispersions were treated at pH = 2 and pH = 5 is probably due to the different residual concentration of quercetin after the first digestion step. At the end of the two-step digestion, about 80% of quercetin was recovered from the two buffers (SGF and SIF). Based on these results, BLG NPs might not be suitable for the controlled release of quercetin in the fed state, but they could release quercetin in a controlled and sustained manner if administrated during the fasting state.

4. Conclusions

In the present paper, encapsulation and quercetin release process of BLG NPs were systematically evaluated. The results showed that acetone anti-solvent had a significant effect on accumulation of BLG NPs. At the acetone content of about 10% v/v, the quercetin loading process had a great influence on EE% and LE% and increased the loading efficacy to about 13.9%. In addition, optimizing the amount of glutaraldehyde and reducing itscontent from 100% to 50% of equivalent led to preparation of low toxic DDS.

The DLS and zeta potential results, after optimizing the initial protein concentration and pH, approved the preparation of nanoparticles with mean particle size of about 180–300 nm and good stability for BLG NPs. Also, the AFM and FESEM images showed semispherical appearance for the NPs. This study suggested that BLG as a resistant protein to peptic digestion could form nanoparticles that were digestible by pepsin at pH = 5, due to breakage of amide bonds that had been formed by glutaraldehyde. As a result, satisfactory controlled release was achieved under simulated fast condition, i.e., digestion in simulated gastric fluid (SGF) at pH = 2 and then in simulated intestinal fluid (SIF).

The results of this study are applicable not only to the BLG-quercetin DDS but also to the other drug delivery systems including water-soluble proteins and hydrophobic compounds with increased satisfactory loading and reduced DDS toxicity.

Acknowledgement

The authors are grateful to Institute of Physics Polish Academy of Sciences, Warsaw, Poland, and University of Isfahan for financial support of this work.

References

Antçnio, E., Khalil, N. M., & Mainardes, R. M. (2016). Bovine serum albumin nanoparticles containing quercetin: Characterization and antioxidant activity. Journal of Nanoscience and Nanotechnology, 16(2), 1346–1353.

Apenten, R. K., Khokhar, S., & Galani, D. (2002). Stability parameters for β-lactoglobulin thermal dissociation and unfolding in phosphate buffer at pH 7.0. Food Hydrocolloids, 16(2), 95–103.

Bengoechea, C., Peinado, I., & McClements, D. J. (2011). formation of protein nanoparticles by controlled heat treatment of lactoferrin: Factors affecting particle characteristics. Food Hydrocolloids, 25(5), 1354–1360.

Benita, S. (2005). Microencapsulation: Methods and industrial applications. Crc Press.

Bhattacharjee, S. (2016). DLS and zeta potential–What they are and what they are not? Journal of Controlled Release, 235(42), 337–351.

Byler, D. M., & Susi, H. (1986). Examination of the secondary structure of proteins by deconvolved FTIR spectra. Biopolymers, 25(3), 469–487.

Cai, X., Fang, Z., Dou, J., Yu, A., & Zhai, G. (2013). Bioavailability of quercetin: Problems and promises. Current Medicinal Chemistry, 20(20), 2572–2582.
Desai, S. J., Singh, P., Simonelli, A. P., & Higuchi, W. I. (1966). Investigation of factors influencing release of solid drug dispersed in inert matrices ii quantitation of procedures. Journal of Pharmaceutical Sciences, 55(11), 1224–1229.
Divsalar, A., Saboury, A., Moosavi-Movahedi, A., & Mansoori-Torshizi, H. (2006). Comparative analysis of refolding of chemically denatured β-lactoglobulin types A and B using the dilution additive mode. International Journal of Biological Macromolecules, 38(1), 9–17.
Duclairoir, C., Nakache, E., Marchais, H., & Orecchioni, A.-M. (1998). formation of gliadin nanoparticles: Influence of the solubility parameter of the protein solvent. Colloid & Polymer Science, 276(4), 321–327.
Dufour, E., & Haertl', T. (1990). Alcohol-induced changes of β-lactoglobulin-retinolbinding stoichiometry. Protein Engineering Design and Selection, 4(2), 185–190.
D'Mello, S. R., Das, S. K., & Das, N. G. (2009). Polymeric Nanoparticles for Small-Molecule Drugs: Biodegradation of Polymers and Fabrications of Nanoparticles. In Y. Pathak, & D. Thassu (Eds.). Drug delivery nanoparticles formulation and characterization (pp. 16–34). New York: Informa Healthcare.
Ezpeleta, I., Irache, J. M., Stainmesse, S., Chabenat, C., Gueguen, J., Popineau, Y., et al. (1996). Gliadin nanoparticles for the controlled release of all-trans-retinoic acid. International Journal Of Applied Pharmacology, 131(2), 191–200.
Fotaki, N., & Vertzoni, M. (2010). Biorelevant dissolution methods and their applications in in vitro-in vivo correlations for oral formulations. Drug Delivery, 4(2), 2–13.
Hertog, M. G., Hollman, P. C., & Katan, M. B. (1992). Content of potentially anticarcinogenic flavonoids of 28 vegetables and 9 fruits commonly consumed in The Netherlands. Journal of Agricultural and Food Chemistry, 40(12), 2379–2383.
He, J.-S., Zhu, S., Mu, T.-H., Yu, Y., Li, J., & Azuma, N. (2011). αs-casein inhibits the pressure-induced aggregation of β-lactoglobulin through its molecular chaperone-like properties. Food Hydrocolloids, 25(6), 1581–1586.
Higuchi, T. (1963). Mechanism of sustained-action medication. Theoretical analysis of rate of release of solid drugs dispersed in solid matrices. Journal of Pharmaceutical

Sciences, 52(12), 1145–1149.
Hixson, A., & Crowell, J. (1931). Dependence of reaction velocity upon surface and agitation. Industrial & Engineering Chemistry Research, 23(8), 923–931.
Invernizzi, G., Annoni, E., Natalello, A., Doglia, S. M., & Lotti, M. (2008). In vivo aggregation of bovine β-lactoglobulin is affected by Cys at position 121. Protein Expression and Purification, 62(1), 111–115.
Jahanshahi, M., Sanati, M., Hajizadeh, S., & Babaei, Z. (2008). Gelatin nanoparticle fabrication and optimization of the particle size. Physica Status Solidi, 205(12), 2898–2902.
Kanakis, C., Hasni, I., Bourassa, P., Tarantilis, P., Polissiou, M., & Tajmir-Riahi, H.-A. (2011). Milk β-lactoglobulin complexes with tea polyphenols. Food Chemistry, 127(3), 1046–1055.
Korsmeyer, R. W., Gurny, R., Doelker, E., Buri, P., & Peppas, N. A. (1983). Mechanisms of solute release from porous hydrophilic polymers. International Journal of Pharmacology, 15(1), 25–35.
Kratz, F., Fichtner, I., Beyer, U., Schumacher, P., Roth, T., Fiebig, H., et al. (1997). Antitumour activity of acid labile transferrin and albumin doxorubicin conjugates in in vitro and in vivo human tumour xenograft models. European Journal of Cancer, 33(2), S175.
Kreuter, J. (1994). Nanoparticles. College Drug Delivery System, 55(6), 219–342.
Lefevre, T., & Subirade, M. (2000). Interaction of β-lactoglobulin with phospholipid bilayers: A molecular level elucidation as revealed by infrared spectroscopy. International Journal of Biological Macromolecules, 28(1), 59–67.
Livney, Y. D. (2010). Milk proteins as vehicles for bioactives. Current Opinion in Colloid & Interface Science, 15(12), 73–83.
Lohcharoenkal, W., Wang, L., Chen, Y. C., & Rojanasakul, Y. (2014). Protein nanoparticles as drug delivery carriers for cancer therapy. BioMed Research International, 2014(22), 189 101.
Marques, M. R., Loebenberg, R., & Almukainzi, M. (2011). Simulated biological fluids with possible application in dissolution testing. Dissolution Technologies, 18(3), 15–28.
Mohammadi, F., Bordbar, A.-K., Divsalar, A., Mohammadi, K., & Saboury, A. A. (2009).

Interaction of curcumin and diacetylcurcumin with the lipocalin member β-lactoglobulin. The Protein J, 28(3–4), 117–123.
Müller, B. G., Leuenberger, H., & Kissel, T. (1996). Albumin nanospheres as carriers for passive drug targeting: An optimized manufacturing technique. Pharmacological Research, 13(1), 32–37.
Nacka, F., Chobert, J.-M., Burova, T., Léonil, J., & Haertlé, T. (1998). Induction of new physicochemical and functional properties by the glycosylation of whey proteins. Journal of Protein Chemistry, 17(5), 495–503.
Najib, N., & Suleiman, M. (1985). The kinetics of drug release from ethylcellulose solid dispersions. Drug Development and Industrial Pharmacy, 11(12), 2169–2181.
Otte, J., Zakora, M., Qvist, K., Olsen, C., & Barkholt, V. (1997). Hydrolysis of bovine β-lactoglobulin by various proteases and identification of selected peptides. International Dairy Journal, 7(12), 835–848.
Patel, B. B., Patel, J. K., Chakraborty, S., & Shukla, D. (2015). Revealing facts behind spray dried solid dispersion technology used for solubility enhancement. Saudi Pharmaceutical Journal, 23(4), 352–365.
Ragona, L., Fogolari, F., Catalano, M., Ugolini, R., Zetta, L., & Molinari, H. (2003). EF loop conformational change triggers ligand binding in β-lactoglobulins. Journal of Biological Chemistry, 278(40), 38840–38846.
Rahimnejad, M., Jahanshahi, M., & Najafpour, G. (2006). Production of biological nanoparticles from bovine serum albumin for drug delivery. African Journal of Biotechnology, 5(20), 1918–1923.
Reddy, I. M., Kella, N. K., & Kinsella, J. E. (1988). Structural and conformational basis of the resistance of β -lactoglobulin to peptic and chymotryptic digestion. Agriculture Food Chemistry, 36(4), 737–741.
Remondetto, G. E., Beyssac, E., & Subirade, M. (2004). Iron availability from whey protein hydrogels: An in vitro study. Agriculture Food Chemistry, 52(26), 8137–8143.
Ricchiuto, P., Rocco, A. G., Gianazza, E., Corrada, D., Beringhelli, T., & Eberini, I. (2008). Structural and dynamic roles of permanent water molecules in ligand molecular recognition by chicken liver bile acid binding protein. Journal of Molecular Recognition, 21(5), 348–354.

Riekes, M. K., Barboza, F. M., Dalla Vecchia, D., Bohatch, M., Jr., Farago, P. V., Fernandes, D., et al. (2011). Evaluation of oral carvedilol microparticles prepared by simple emulsion technique using poly (3-hydroxybutyrate-co-3-hydroxyvalerate) and polycaprolactone as polymers. Materials Science and Engineering: C, 31(5), 962–968.

Sahihi, M., Bordbar, A.-K., Ghayeb, Y., & Fani, N. (2012). Structure–function relationship of β-lactoglobulin in the presence of sodium dodecylbenzenesulfonate. Journal of Chemical Thermodynamics, 52(10), 16–23.

Sahihi, M., Ghayeb, Y., & Bordbar, A.-K. (2012). Fluorescence spectroscopic study on interaction of retinol with β-lactoglobulin in the presence of cetylpyridinium chloride. Journal of Spectroscopy, 27(1), 27–34.

Sahihi, M., Ghayeb, Y., & Bordbar, A.-K. (2013). Interaction of β-lactoglobulin with resveratrol: Molecular docking and molecular dynamics simulation studies. Chemical and Biochemical Engineering Quarterly, 27(4), 417–422.

Sahu, A., Kasoju, N., Goswami, P., & Bora, U. (2011). Encapsulation of curcumin in Pluronic block copolymer micelles for drug delivery applications. Journal of Biomaterials Applications, 25(6), 619–639.

Surewicz, W. K., & Mantsch, H. H. (1988). New insight into protein secondary structure from resolution-enhanced infrared spectra. Biochimica et Biophysica Acta, 952(20), 115–130.

Teng, Z., Li, Y., Luo, Y., Zhang, B., & Wang, Q. (2013). Cationic β-lactoglobulin nanoparticles as a bioavailability enhancer: Protein characterization and particle formation. Biomacromolecules, 14(8), 2848–2856.

Teng, Z., Li, Y., & Wang, Q. (2014). Insight into curcumin-loaded β-lactoglobulin nanoparticles: Incorporation, particle disintegration, and releasing profiles. Journal of Agricultural and Food Chemistry, 62(35), 8837–8847.

Teng, Z., Luo, Y., & Wang, Q. (2012). Nanoparticles synthesized from soy protein: Preparation, characterization, and application for nutraceutical encapsulation. Journal of Agricultural and Food Chemistry, 60(10), 2712–2720.

Teng, Z., Luo, Y., Wang, T., Zhang, B., & Wang, Q. (2013). Development and application of nanoparticles synthesized with folic acid conjugated soy protein. Journal of Agricultural and Food Chemistry, 61(10), 2556–2564.

Tønnesen, H. H., & Karlsen, J. (1985). Studies on curcumin and curcuminoids. Zeitschrift für Lebensmittel-Untersuchung und -Forschung, 180(5), 402–404.
Vandervoort, J., & Ludwig, A. (2004). Preparation and evaluation of drug-loaded gelatin nanoparticles for topical ophthalmic use. European Journal of Pharmaceutics and Biopharmaceutics, 57(2), 251–261.
Wang, Q., Allen, J. C., & Swaisgood, H. E. (1997). Binding of vitamin D and cholesterol to β-lactoglobulin. Journal of Dairy Science, 80(6), 1054–1059.
Weber, C., Coester, C., Kreuter, J., & Langer, K. (2000). Desolvation process and surface characterisation of protein nanoparticles. International Journal of Pharmacy, 194(1), 91–102.
Wu, T.-H., Yen, F.-L., Lin, L.-T., Tsai, T.-R., Lin, C.-C., & Cham, T.-M. (2008). Preparation, physicochemical characterization, and antioxidant effects of quercetin nanoparticles. International Journal of Pharmacy, 346(1–2), 160–168.
Yun, Y., Cho, Y. W., & Park, K. (2013). Nanoparticles for oral delivery: Targeted nanoparticles with peptidic ligands for oral protein delivery. Advanced Drug Delivery Reviews, 65(6), 822–832.
Zhang, X., Li, L., Xu, Z., Liang, Z., Su, J., Huang, J., et al. (2013). Investigation of the interaction of naringin palmitate with bovine serum albumin: Spectroscopic analysis and molecular docking. PLoS One, 8(3), 59106.